Journal of Applied Polymer Science

Development of Fibrin Conjugated Chitosan/Nano β-TCP Composite Scaffolds with Improved Cell Supportive Property for Bone Tissue Regeneration

Nadeem Siddiqui, Krishna Pramanik
Department of Biotechnology and Medical Engineering, National Institute of Technology, Rourkela, India 769008
Correspondence to: K. Pramanik (E-mail: kpr@nitrkl.ac.in)

ABSTRACT: In the present study, an attempt has been made to improve cell supportive property of chitosan/nano beta tri-calcium phosphate (β-TCP) composite scaffolds by modification of scaffold surface with fibrin using ethyl-3-(3-dimethylaminopropyl) carbodimide (EDC) as crosslinking agent. The developed fibrin conjugated chitosan/nano β-TCP composite scaffolds possess desired pore size and porosity in the range of 45–151 μm and 81.4 ± 4.1%, respectively. No significant change in compressive strength of scaffolds was observed before and after fibrin conjugation. The calculated compressive strength of fibrin conjugated and non-conjugated chitosan/nano β-TCP scaffolds are 2.71 ± 0.14 MPa and 2.67 ± 0.11 MPa, respectively. Results of cell culture study have further shown an enhanced cell attachment, cell number, proliferation, differentiation, and mineralization on fibrin conjugated chitosan/nano β-TCP scaffold. The uniform cell distribution over the scaffold surface and cell infiltration into the scaffold pores were assessed by confocal laser scanning microscopy. Furthermore, higher expression of osteogenic specific genes such as bone sialo protein, osteonectin, alkaline phosphatase, and osteocalcin (OC) on fibrin conjugated scaffolds was observed when compared to scaffolds without fibrin. Altogether, results indicate the potentiality of developed fibrin conjugated composite scaffolds for bone tissue engineering applications. © 2014 Wiley Periodicals, Inc. J. Appl. Polym. Sci. **2015**, *132*, 41534.

KEYWORDS: biocompatibility; biodegradable; biomaterials; composites; degradation

Received 21 May 2014; accepted 17 September 2014
DOI: 10.1002/app.41534

INTRODUCTION

Bone tissue defects and diseases due to trauma, injuries, infections, and degeneration are a major human health concern. Tissue engineering seems to be a new hope in treating these bone-related defects and diseases.[1] In tissue engineering, development of 3D scaffold matrix from a biocompatible and biodegradable material is the key for the success of any tissue engineered graft.[2] In this context, natural biopolymers are considered as ideal scaffold materials for bone tissue regeneration. Among natural biomaterials, chitosan seems to be an attractive candidate due to its excellent biocompatibility, biodegradability, and innate antibacterial property.[3] However, the major drawback of chitosan is that it lacks mechanical strength for hard tissue engineering applications. Several researchers attempted to improve the mechanical property of chitosan by incorporating a variety of bio-ceramics such as wollastonite, hydroxy apatite, beta tri-calcium phosphate (β-TCP), and by crosslinking with various natural/chemical crosslinkers.[4–6] Nanosized ceramics has further improved the mechanical strength of scaffolds compared to microsized ceramic particles. Reinforcement of nanohydroxyapatite (nHAp) particles into chitosan matrix has not only increased the mechanical strength but also decreased degradation rate of chitosan by 10%.[4] β-TCP confirms its excellent biocompatibility, osteoconductivity, and favors cell growth, proliferation, and differentiation of mesenchymal stem cells (MSCs). Incorporation of β-TCP has enhanced the compressive strength of chitosan scaffold to 1.8 MPa by freeze gelation method.[5] In our previous work, an increased mechanical and bioactivity of chitosan (CS) scaffold was also achieved by the incorporation of micro- and nanosized β-TCP using freeze gelation method.[6] Biostability of collagen/chitosan hydrogels was significantly increased by carbodimide crosslinking and noticed an increase in mechanical strength and elasticity of hydrogels to 10 and 20%, respectively. Further, ethyl-3-(3-dimethylaminopropyl) carbodimide (EDC) treated hydrogels were successfully implanted in cornea of pigs for 12 months and found excellent regeneration of host corneal epithelial cells around the implanted site.[7] Surface functionalized CS composite scaffolds are promising for their tissue engineering applications and hence research has been focused on proper surface modification of CS-based scaffolds to improve cell supportive property. It is further reported that biologically

modified surface is superior to chemical modification which affects the integration of proteins, peptides, and nucleic acids.[8] Fibrin has been used since a very long time in tissue engineering applications like wound healing, as an angiogenic factor, and to improve differentiation ability of osteogenic cells.[9] The ability of fibrin to mold into different forms as glue, sealant, and adhesive makes it a special natural biomaterial. Porous structures obtained with fibrin were also reported to deliver growth factors like vascular endothelial (VEGF) and fibroblast growth factor (bFGF).[10] However, the major handicap of fibrin is its fragile nature and rapid degradation which limits its use in bone tissue engineering applications.[11] Surface functionalization with a proper method is of paramount importance for CS composites to be used in biological system. In this context, crosslinkers like EDC and *N*-hydroxysuccinimide (NHS) were widely used to conjugate fibrin/arginyl glycyl aspartic acid (RGD) with polymeric materials due to their low toxicity.[12] There are few reports on surface medication of CS by UV crosslinking to conjugate fibrin and RGD peptide immobilization which improved cell adhesive property of chitosan scaffolds.[13] Published reports proved that the presence of RGD peptide sequences in the fibrin provides numerous cell adhesion sites making it special in overcoming the cell seeding defects and thus promoting excellent tissue growth.[14] Fibrin is also famous for its supportive role in angiogenesis and differentiation of seeded MSCs.[15] The novelty of the present work lies in fibrin conjugation with the help of carbodimide crosslinking to improve low cell binding ability of chitosan/nano β-TCP composite scaffolds. Various physico-chemical properties of developed scaffolds were investigated. Further, cytocompatibility of these scaffolds was evaluated by seeding human MSCs isolated from umbilical cord. Confocal laser scanning microscopy was done to trace the distribution and infiltration of cells and cytoskeleton organization. Finally, semi quantitative reverse transcription polymerase chain reaction (RT-PCR) was performed to examine the relative expression of osteogenic markers at 21 days of culture. Due to synergic effects of β-TCP and fibrin, the developed scaffolds have shown superior qualities in terms of mechanical strength and biocompatibility.

EXPERIMENTAL

Materials

Chitosan (190 kDa with 85% degree of deacetylation), nano β-TCP powder, fibrinogen, prothrombin, lysozyme, EDC, NHS, 2-(morpholino) ethane sulfonic acid (MES), sodium chloride (NaCl), pottasium chloride (KCl), calcium chloride ($CaCl_2$), magnesium chloride ($MgCl_2$), pottasium dihydrogen phosphate (K_2HPO4),sodium bicarbonate ($NaHCO_3$), and di sodium sulphate (Na_2SO_4) were procured from Sigma Aldrich Chemicals (USA). Di sodium hydrogen phosphate (Na_2HPO_4), sodium hydroxide (NaOH) pellets, acetic acid (CH_3COOH), and ethanol (C_2H_5OH) were purchased from Merck (India) and used without any further purification.

Preparation of Chitosan/nano β-TCP Composite Scaffolds

Chitosan/nano β-TCP composite scaffolds were prepared according to the previous reported method.[16] Briefly, 2.5 g of chitosan was dissolved in aqueous acetic acid (0.1*M*) to form chitosan solution. About 0.4 wt % nano β-TCP powder was suspended in water, sonicated, and added drop wise to the prepared chitosan solution. The solution was stirred for 12 h at room temperature. The solution was then poured into molds and kept at $-20^{\circ}C$ for 4 h. The frozen molds were immersed in a mixture of pre chilled NaOH : EtOH of 70 : 30 (vol/vol) for 6 h. The molds were removed from NaOH : EtOH mixture and vacuum dried for 4 h at 40°C. Scaffolds were rinsed with deionized water thrice and finally dried. Similarly, pure CS scaffolds were prepared and used as control.

Preparation of Fibrin Conjugated CS/Nano β-TCP Composite Scaffolds

CS/nano β-TCP composite scaffolds were crosslinked with EDC/NHS solution at 105°C for 24 h prior to fibrin conjugation following the procedure described in published literature.[17] The scaffolds were washed with double-distilled water for three times (10 min each) followed by drying to obtain EDC/NHS treated CS/nano β-TCP composite scaffolds. Fibrin was conjugated to EDC treated CS/nano β-TCP composite scaffolds following the procedure described elsewhere.[12] Briefly, crosslinked scaffolds were sterilized in 75% ethanol overnight followed by a phosphate buffered saline (PBS) wash. About 50 $\mu L/cm^2$ of fibrinogen (80 mg/mL) and 50 $\mu L/cm^2$ of thrombin (600 U/mL) solutions were spread on the surface of CS/nano β-TCP scaffolds and kept for incubation at 37°C for 30 min till fibrin glue forms on the surface of the composite scaffolds.

Characterization

Morphological Analysis. Morphology of prepared scaffolds was assessed by scanning electron microscope (SEM JEOL-JSM6480LV, Japan). Gold coating (Quorumtech, Q150RES, Czech Republic) was done on the sample surface prior to imaging for 2 min. Images were collected at 15 kV. A minimum of 25 pores were considered for calculating the pore size of the developed scaffolds by using Image J (USA) software.

Phase Analysis. Phase analysis of prepared scaffolds was performed by X-ray diffractometer (Ultima IV, Rigaku, Japan) equipped with a Cu-K alpha tube to generate X-rays. Samples were scanned in a 2θ range of 5°–80° with a scanning speed of 2° per minute.

Structural Analysis. Fourier transform infrared spectroscopy (FTIR, Shimadzu AIM-8800, Japan) was performed to study the chemical characteristics of developed scaffolds. Samples were pelletized with 300 mg of KBr powder by hydraulic press.[18] The machine was operated to run in transmittance mode with a spectral resolution of 8 cm^{-1} from 500 to 4000 cm^{-1}.

Porosity. Porosity of the prepared scaffolds was analyzed by mercury intrusion porosimeter (Poremaster-33, Quantachrome, USA). The bulk density of samples was calculated by equation, $B.D = D/W - S$, where D = dry weight, S = suspended Weight, W = soaked weight. The % porosity was obtained by mercury intrusion data according to Washburn equation.[19]

Mechanical Property. Compressive strength of prepared scaffolds was measured by Universal testing machine (H10 KS Tinius Olsen USA). Cylindrical samples with a diameter of 10 mm and thickness of 8 mm were used for analysis.[20] Compression test was performed with a crosshead speed of 1 mm/min with a load cell of

1000 N. Each scaffold sample was tested in triplicate. Compressive strength was calculated using the formula $S=F_{max}/A$, in which F_{max} represents the force applied and A is the cross-sectional area of the sample.

Degradation Study. Simulated body fluid (SBF) consisting of lysozyme (500 μg mL^{-1}) was used to assess the degradation of developed scaffolds according to protocol published elsewhere.[21] The initial dry weight of the samples were measured and noted as W_o. The samples were immersed in 15 mL of SBF and kept for predetermined time intervals of time (1, 7, 14, 21, and 28 days) with gentle mechanical agitation at 37°C. Samples were collected from SBF at each time point, rinsed with water, and weighed. Then the samples were freeze dried, weighed, and noted as W_t. The remaining weight percentage (W_R) was calculated according to the formula (by using Mathtype 5.0) given below.

$$\%\ \text{Weight remaining} = 100 - [(W_o - W_t)/W_o \times 100] \quad (1)$$

Contact Angle Measurement. The contact angle of the developed scaffolds was measured by a tensiometer (K100MK3 Kruss, Germany) by following the published protocol.[22] Water was used as the solvent for accomplishing the measurements with a detection speed of 6 mm/min. The scaffolds with a dimension of 9 mm × 12 mm × 5 mm were used for the analyses. The mean value of contact angles was calculated from three individual measurements at 25°C and 65% humidity.

In Vitro Cell Study

Cell Culture and Seeding. Umbilical cord blood was used to isolate MSCs and maintained in Dulbecco's modified Eagle's medium (Gibco, USA) consisting of 10% fetal bovine serum (FBS) and 1% antibiotic solution. Cells were subcultured in tissue culture flasks till 4th passage at room temperature with 5% of CO_2 in a humidified atmosphere of 95% air.[23] Cells were detached using 0.05% trypsin containing 1 m*M* EDTA (Sigma Aldrich). Cells were seeded on sterilized (70% ethanol treatment for 2 h, followed by PBS wash) scaffolds by static method with a seeding density of 5×10^6 cells/mL. The cell seeded scaffolds were incubated in osteogenic media (DMEM supplemented with 10% FBS, 10 n*M* Dexamethasone, 10 m*M* β-glycero phosphate, and 0.28 m*M* ascorbic acid). The media was replaced at regular interval of 3 days.

Cell Attachment and Morphology. Cell attachment and spreading on the scaffold was observed by field emission microscope (FE-SEM, Nova SEM450-Czech Republic). About 2% (vol/vol) gluteraldehyde (Sigma, USA) solution was used for fixing the cells. Samples were rinsed with wash buffer thrice and a gradient of ethanol wash was done and finally air dried.[19] Cell scaffold constructs were gold sputter coated (Quorumtech, Q150RES, Czech Republic) prior to imaging. Images were collected by operating FE-SEM in high vacuum at 30 kV for morphological assessment of seeded cells.

MTT Assay. The metabolic activity of cell seeded scaffolds was analyzed by MTT (3-(4,5-dimethylthiazol-2-y1)−2,5-diphenyltetrazolium bromide assay (Sigma, USA) according to the procedure reported earlier.[24] Briefly, 10 μL of MTT solution (5 mg/mL) was added to the cultured MSCs and culture plate was incubated at 37°C for 4 h. Dimethyl sulfoxide (DMSO) (Invitrogen) of 100 μL was used to solubilize formazan and absorbance was measured at 595 nm in a microplate reader (2030 multi label reader Victor X3, Perklin Elmer, USA).

Cell Proliferation Assay. Proliferation of hMSCs on cell seeded scaffolds was assessed by DNA quantification assay at predetermined time points of 3, 7, 14, and 21 days culture. Cells were washed with PBS (Invitrogen) and followed by cell lysis using 0.5 mL of 0.2% Triton X-100 (Invitrogen). Assay was performed based on published protocol.[25] Alkaline lysis method was used to extract cellular DNA from cell-scaffold constructs. The absorbance of extracted DNA was measured by microplate reader at 260 nm. (2030 multi label reader Victor X3, Perklin Elmer,USA).

Osteogenic Differentiation of MSCs Seeded on Developed Scaffolds

The osteogenic differentiation of MSCs over the scaffolds was evaluated by alkaline phosphatase (ALP), mineralization assay, and quantifying the relative expression of osteogenic markers which are described below.

ALP Assay. ALP activity of scaffolds was performed by using Quanti Chrom Alkaline Phosphatase Assay Kit (BioAssay Systems) according to manufacturer's protocol.[24] In brief, the scaffolds cultured in osteogenic differentiation media for 7, 14, and 21 days were collected and rinsed with PBS. Cells were lysed using 0.5 mL of 0.2% Triton X-100 and then sonicated. About 190 μL of working solution having *p*-nitro phenol phosphate was added to the 10 μL cell lysate and incubated for 4 min at 37°C. The absorbance was measured at 405 nm using a micro plate reader (2030 multi label reader Victor X3, Perklin Elmer, USA) at initial time point and at 4 min. ALPase activity was calculated according to the following equation.

$$O.D_{t=4} - O.D_{t=0}/O.D_{\text{calibrator}} - O.D_{\text{ddH}_2\text{O}} \quad (2)$$

***In Vitro* Mineralization Assay.** Alizarin red assay was used to quantify the mineralization of hMSCs on the developed chitosan-based composite scaffolds based on the previously reported protocol.[26] hMSCs seeded scaffolds were washed with PBS and fixed with 4% paraformaldehyde for 20 min. Then the scaffolds were washed thoroughly with distilled water. About 400 mL of Alizarin red stain (40 m*M* pH 4.1; Sigma, USA) was added and the samples were incubated at room temperature for 10 min. In order to itemize the mineralization, alizarin red stain was removed from the scaffold by 500 μL of cetylpyridinium chloride for 1 h. Images were collected using optical microscope.

Expression of Osteogenic Specific Genes: Semi Quantitative RT-PCR Analysis. Primer sequences used for the study were procured from Sigma Aldrich (USA) and shown in Table I. For RT-PCR analysis, the total cellular RNA from osteoblasts (differentiated from hMSCs) was extracted by TRIzol (Gibco, USA). Synthesis of cDNA was carried out using first strand cDNA synthesis kit (Fermentas) following the manufacturer's protocol. The synthesized cDNA was used as a template for the semi-quantitative RT-PCR following the procedure followed elsewhere.[27] The β-actin gene was used as a housekeeping gene for normalizing mRNA level of ALP, osteo calcin (OC), osteonectin (ON), bone sialo protein (BSP), and collagen type I (Col-I)

Table I. RT-PCR Primers Used for Expression of Osteogenic Specific Genes

Gene	Direction	Primer sequence
β-actin	Forward	5′-TCTACAATGAGCTGCGTGTG-3′
	Reverse	5′-CAACTAAGTCATAGTCCGCC-3′
Bone Sialo protein (BSP)	Forward	5′-CTTACCGAGCTTATGAGGATGAATA-3′
	Reverse	5′-ATTGGGAAGCAGAAAGATTAGATG-3′
Osteonectin (ON)	Forward	5′-CAC TGG CGC TGC AACAAG A-3′
	Reverse	5′-CAT TCC GGA GCT CAGCAG AAT-3′
Alkaline phosphatase (ALP)	Forward	5′-GGG GGT GGC CGG AAATAC AT-3′
	Reverse	5′-GGG GGC CAG ACC AAAGAT AG-3′
Osteocalcin (OC)	Forward	5′-CCC AGG CGC TAC CTGTAT CAA-3′
	Reverse	5′-GGT CAG CCA ACT CGTCAC AGTC-3′
Collagen I (Col I)	Forward	5′-GGCAATAGCAGGTTCACGTACA-3′
	Reverse	5′-CGATAACAGTCTTGCCCCACTT-3′

gene. The PCR reaction mixture consists of 1X PCR buffer, 50 m*M* $mgCl_2$, 10 m*M* dNTPs, 0.2 μ*M* of each primer, 1 U Taq polymerase, and autoclaved water. PCR chain reactions were performed at 94°C for 2 min, 35 cycles 96°C for 30 s, 55–63°C for 45 sec, and 72°C for 45 s and 72°C for 10 min. Finally, the amplified DNA fragments (PCR products) were subjected to electrophoresis on 1.5% agarose gel and the band intensities were measured using Image J (USA) software.

Cell Distribution and Cytoskeletal Organization

Cell distribution and cytoskeletal organization on cell seeded scaffolds were analyzed by confocal laser scanning microscope (CLSM Leica SP8 inverted microscope, Germany) by using Hoescht (Invitrogen) and Alexa Floor 488 Phalloidin (Invitrogen) according to the protocol followed elsewhere.[28] Briefly, cultured cell scaffold constructs (14th day) were fixed with 4% paraformaldehyde (Sigma, USA) for 1 min followed by Hoescht nuclear staining for 1 min each. Prior to stain F-actin, the cell scaffold constructs were fixed with 3.7% paraformaldehyde for 10 min followed by permeabilization with Triton-X for 5 min and then blocked with PBS containing 1% bovine serum albumin (BSA) for 30 min. Finally, the constructs were stained with Phalloidin conjugated to Alexa Floor and the samples were examined by using confocal laser scanning microscope at excitation wavelengths of 488 and 633 nm. Images were collected in z-stack mode with optical sectioning at 0.2 μm and were converted to 3D images in Leica LAS AF lite software to visualize distribution of cells inside the scaffold.

Statistical Analysis

Statistical analysis of the results obtained for the different groups of scaffolds at various conditions was performed by using student's *t*-test. Most of the results (mechanical, contact angle, MTT, DNA quantification, and ALP assay) were obtained from triplicate samples. Degradation and porosity experiments were performed twice to get significant results. *P* value less than < 0.05 was considered statistically significant.

RESULTS AND DISCUSSION

Preparation of Scaffold

Fibrin conjugated CS/nano β-TCP scaffold was successfully prepared by crosslinking with EDC. Figure 1 shows the schematic representation of fibrin conjugation to CS/nano β-TCP scaffolds through EDC crosslinking. The developed scaffolds are designated as pure CS scaffolds, chitosan/nano β-TCP composite scaffolds (CS/n β-TCP), and fibrin conjugated scaffolds (CS/n β-TCP/F).

Morphological Analysis

Pore size and porosity of scaffolds are important factors for efficient cell migration and transport of nutrients to cells.[29] SEM micrographs as depicted in Figure 2(A) reveal an open and interconnected porous network of the fibrin conjugated scaffold that is similar to the non-conjugated CS/nano β-TCP scaffold.[6] The pore size of the scaffold is measured as 45–151 μm which is slightly lower than CS/nano β-TCP (55–162 μm) and pure CS scaffolds (61–171 μm). The slight decrease in pore size as compared to control may be attributed to the crosslinking by EDC-NHS. The decrease in pore size is also reported when CS matrices was crosslinked with carbodimide for corneal tissue engineering applications.[7] However, the obtained pore size range of fibrin conjugated CS/nano β-TCP is adequate for hosting the seeded cells, cell adhesion to the inner surface, and diffusion of nutrients through the scaffold. The fibrillar structure of fibrin on the scaffold surface is evident from SEM image which is advantageous for the diffusion of water soluble substances to the cells through the porous architecture of composite scaffolds.

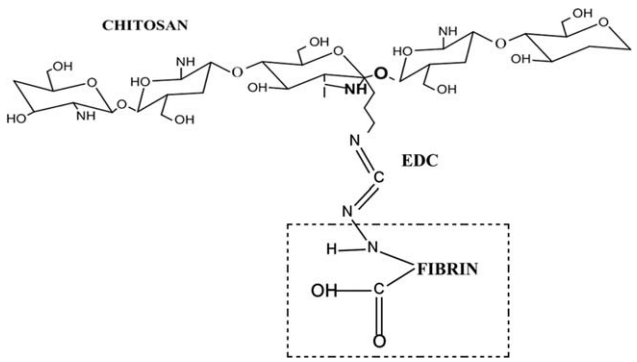

Figure 1. Schematic representation of Fibrin conjugation to chitosan based composite scaffolds using EDC molecule.

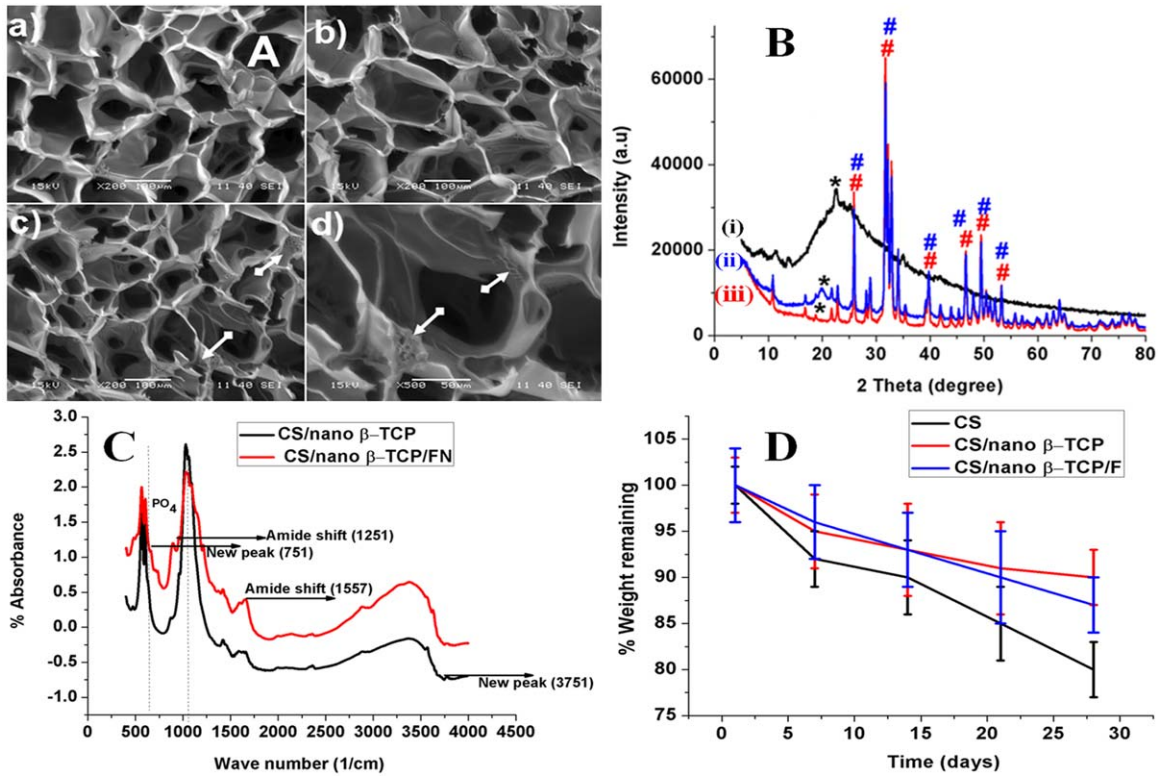

Figure 2. Morphology (A), Phase (B), Functional (C), and Percentage weight remaining (D) of Fibrin conjugated and non-conjugated scaffolds. [Color figure can be viewed in the online issue, which is available at wileyonlinelibrary.com.]

It has also been reported that the microstructure of fibrin conjugated scaffolds plays dual role by providing suitable porous platform to the cells and the micro channels formed offer efficient transport of nutrients from the media to the cultured cells.[11] Furthermore, the rough surface of fibrin conjugated scaffolds is favorable for improving cellular responses.

Phase Analysis

Figure 2(B) shows X-ray diffraction patterns of developed scaffolds. Prominent sharp peaks at $2\theta = 31.1°$ and 34.4° confirms the presence of β-TCP in fibrin conjugated and non-conjugated composite scaffolds.[30] There is a decrease in the intensity of CS peak (amorphous nature) in both types of scaffold. However, the decrease in the intensity of CS peak is slightly higher in fibrin conjugated scaffolds as compared to non-conjugated scaffolds which is attributed to the effective crosslinking.[31]

Structural Analysis

An infrared spectrum signifies the interactions between individual components of a composite system and thus helps in identification of chemical constituents.[30] Figure 2(C) illustrates the bands observed in the IR spectra for CS/nano β-TCP and CS/nano-β TCP/F scaffolds. Bands at 1040, 1122, 610, and 551 cm^{-1} correspond to PO_4^{-3} of β-TCP.[5] It has been reported that shifting as well as generation of new peaks occur due to chemical interactions between individual components of composite scaffolds.[7] The amide II and amide III absorption bands at 1550 and 1240 cm^{-1} belonging to fibrin protein have been shifted to 1577 cm^{-1} and 1251 cm^{-1}.[9] New bands at 751 cm^{-1} and 3751 cm^{-1} is seen in non-conjugated and conjugated scaffolds which may be due to the interactions between PO_4^{-3} with C═O of fibrin and N─H of CS, respectively.

Porosity

A slight increase in porosity is obtained with the fibrin conjugated composite scaffold compared to composite scaffold without fibrin. The porosity of CS/nano β-TCP composite scaffolds conjugated with fibrin is 81.4 ± 4.1 whereas that of non-conjugated scaffold is 80.1 ± 3.60. This slight increase in porosity of fibrin conjugated scaffold may be as a result of reduced pore size caused due to EDC crosslinking. Both conjugated and non-conjugated scaffolds have shown decreased % porosity as compared to pure CS—86% which is statistically significant at $P < 0.05$. Similar trend in porosity was also observed in previous study where the porosity of gelatin scaffolds has been reported to slightly increase due to crosslinking with glutaraldehyde.[32] Published reports have recommended a pore size and porosity range of 30–300 μm and 70–90% respectively for successful bone tissue engineering and our results correlates the same.[33]

Mechanical Property

The mechanical strength of a scaffold influences various cellular activities like proliferation and differentiation.[16] No significant increase in compressive strength is observed with fibrin conjugated scaffold. The mechanism of crosslinking between EDC with CS involves the reaction between amino and carboxylic groups.[34] As CS does not possess any carboxylic groups in its chain, the crosslinking reaction is weak and hence no significant change in compressive strength of scaffold is observed. However,

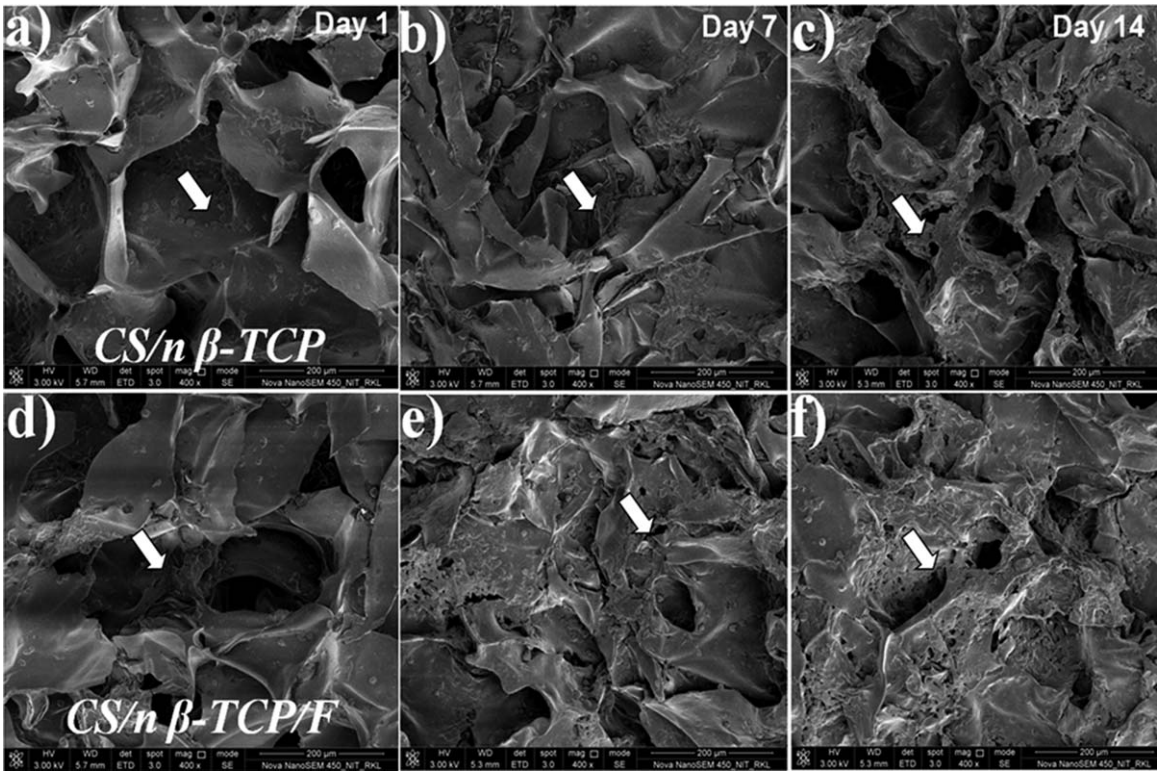

Figure 3. FE-SEM images showing morphological changes an attachment of hMSCs on CS/nano β-TCP (a–c) and CS/nano β-TCP/F composite scaffolds (c–e) during 14-day culture period. Images depict the morphological changes of hMSCs. Spherical shape (a, d) on day 1, colonization (b, e) on day 7, and well spreading sheet-like structures (e, f) on day 14.

both conjugated (2.71 ± 0.14 MPa) and non-conjugated (2.67 ± 0.21 MPa) scaffolds have shown higher compressive strength as compared to pure CS scaffold $-0.1\ 9 \pm 0.05$ MPa ($P < 0.05$).

Biodegradation

The degradation of scaffolds is one of the major goal of tissue engineering research because the self-repairing ability of various tissues are different implying that scaffold should have corresponding degradation rates to facilitate neo tissue synthesis.[35] The degradation study was performed by the treatment of scaffold in SBF containing lysozyme. Lysozyme helps in the hydrolytic scission of glycosidic links present between CS units leading to smaller length chains thereby degradation of scaffold occurs.[36] Figure 2(D) represents the *in vitro* degradation pattern of developed scaffolds. Fibrin conjugated CS/nano β-TCP scaffold degraded to ~14% where as CS/nano β-TCP composite scaffold degraded to ~16% ($P > 0.05$). Both fibrin conjugated and non-conjugated scaffolds have shown a lower degradation rate than pure CS scaffold 31% ($P < 0.05$). The slight lower degradation rate observed with CS/nano β-TCP/F composite scaffold is attributed to enhanced compactness and rigidity of the polymer matrix due to EDC crosslinking. Further, as CS is more hydrophilic compared to CS/nano β-TCP and fibrin conjugated CS/nano β-TCP composite scaffolds, it allows more SBF to diffuse through its matrix which results in faster degradation. β-TCP reinforced scaffolds takes more time to degrade as compared to pure CS which may be due to decrease in pore size, porosity, water retention ability and increased crystallinity of composite scaffold. Similarly, wollastonite, HAp incorporation has decreased the rate of degradation by 15% when they were subjected SBF degradation.[18,37] The fibrillar network of fibrin restricts diffusion of SBF into the porous architecture of fibrin conjugated scaffold thereby a decrease in degradation rate of fibrin conjugated scaffolds is observed. Furthermore, the crosslinking of scaffolds provide resistance to biodegradation due to increase in inter- and intra-molecular hydrogen bonds.[38] The scaffold with lower degradation is favorable to provide support to the growing cells for a certain longer period of time. This may be of a greater importance in *in vivo* handling of transplanted scaffold. Previous reports suggest that optimal degradation of scaffolds eases the longevity of scaffold implantation at tissue damaged site.[39] DTBP (Di methyl 3,3 dithiopropionimidate) crosslinked CS scaffolds well maintained their structural integrity and degraded to 10% only during 21 days of incubation.[40]

Contact Angle Measurement

The hydrophilicity of the scaffold is important with respect to the protein adsorption on the surface of any implant.[41] From the assay result, no significant change is noticed between the contact angles of pure CS ($51.2 \pm 0.8°$), CS/nano β-TCP ($51.9 \pm 1.1°$) and fibrin conjugated CS/nano β-TCP composite scaffolds ($53.1 \pm 0.5°$). Therefore, the hydrophilicity of developed scaffolds is comparable and the slight variation in contact angle exhibited by fibrin conjugated scaffold is attributed to the extent of crosslinking and variation in porosity.[22]

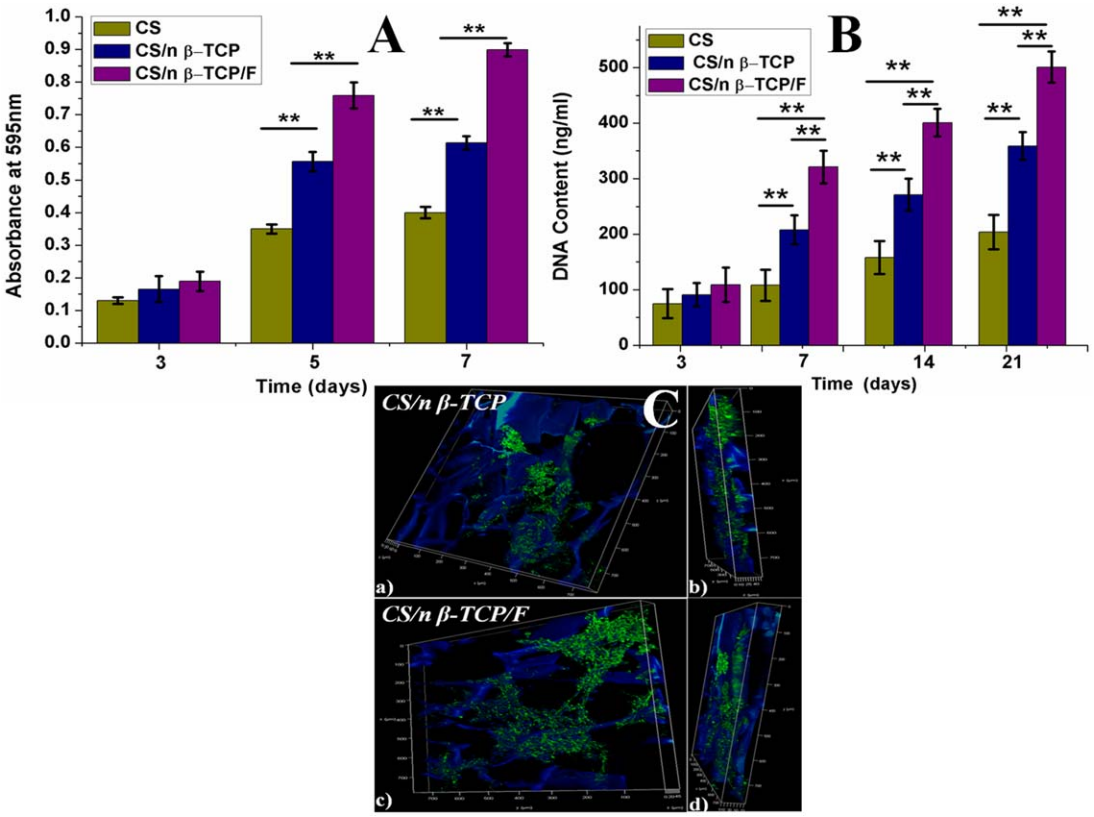

Figure 4. MTT assay (A) of hMSCs seeded on fibrin conjugated and non-conjugated composite scaffolds on 3, 5, and 7 days of culture. Cell proliferation (B) represented in terms of DNA quantification on developed scaffolds upto 21 days of culture. Fibrin conjugated scaffold has shown highest proliferation at any time point. 3D laser scanning confocal images (C) of hMSC morphology after 14 days of culture on CS/nano β-TCP (a, b) and CS/nano β-TCP/F composite scaffolds (c, d). Nuclei of the cells are stained with Hoechst 33342 (blue) and actin filaments with phalloidin (green). [Color figure can be viewed in the online issue, which is available at wileyonlinelibrary.com.]

In Vitro Cell Study

Cell Attachment and Morphology. Cell attachment and morphology of MSCs seeded on the scaffolds were observed in Figure 3. On close observation, MSCs were found to attach, spread, and migrate over the scaffold surface over the culture period. Cell attachment on the scaffolds was visualized using FE-SEM and is depicted in Figure 3(a–f). On day 1, cells are found to be spherical in shape and appear individually [Figure 3(a,d)] whereas cells grew well over the scaffold surface on day 7 and 14, resembling a sheet-like structure due to rapid spreading [Figure 3(c,f)]. Cells were also found to appear as aggregates at later time points as represented in Figure 3(b,c,e,f). Thus we conclude from FE-SEM study that the number of cells attached and proliferated on fibrin conjugated scaffolds is significantly higher when compared to non-fibrin conjugated scaffolds suggesting superior cytocompatibility of CS/nano β-TCP/F scaffolds.

MTT Assay. Metabolic activity of the MSCs seeded on the prepared scaffolds was examined by MTT assay. Figure 4(A) shows increased cell viability at each time point. After 7 days of incubation, higher cell viability is achieved on CS/nano β-TCP/F composite scaffolds compared to pure CS and CS/nano β-TCP composite scaffolds. A significant increase in metabolic activity is observed between CS and CS/nano β-TCP/F composite scaffold groups ($P < 0.05$). This increase in metabolic activity can be attributed to the presence of RGD sequences in fibrin which provides suitable cell recognition sites to attract more number of cells on the scaffold surface.[42] Thus it is established that fibrin conjugation can enhance cell proliferation on scaffolds as reported earlier.[14]

Cell Proliferation Assay

The proliferation of MSCs on the prepared scaffold was further evaluated by DNA quantification assay. Figure 4(B) shows an increase in DNA content with time in all the developed scaffolds with varying degree of cell proliferation. Cell recognition binding sites or specific peptides like RGD on the surface of scaffold matrices enhance cell polymer interactions as reported earlier.[4] Throughout the culture period, CS/nano β-TCP/F composite scaffold scaffolds show higher DNA content (501 ± 24 ng/mL) than CS (204 ± 9 ng/mL) and CS/nano β-TCP composite scaffold (289 ± 16 ng/mL) representing the enhanced proliferation rate achieved with CS/nano β-TCP/F. Thus the fibrin conjugated scaffolds is proved to mimic the native environment in a better way that support the growth and proliferation of hMSCs as compared to other CS scaffolds.

Cell Distribution and Cytoskeleton Organization

It is important to know the cell distribution in the inner sections of 3D scaffold for understanding the cell penetration

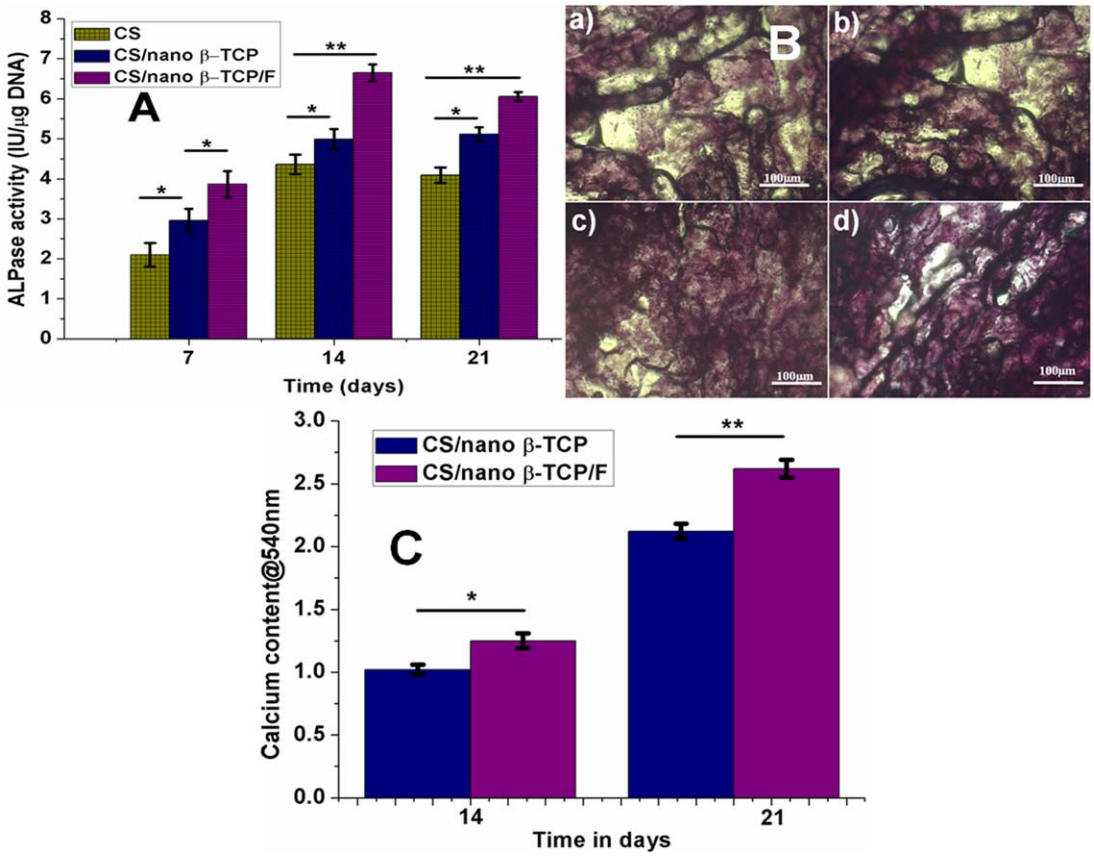

Figure 5. ALP activity (A) of hMSCs cultured on pure CS, fibrin conjugated and non-conjugated CS/nano β-TCP composite matrices after 21 days of culture. Optical microscopy images (B) for CS/nano β-TCP (a, b) and CS/nano β-TCP/F (c, d) composite scaffolds. Quantitative representation (C) of mineral deposition on CS/nano β-TCP and CS/nano β-TCP/F composite scaffolds upto 21 days of incubation. [Color figure can be viewed in the online issue, which is available at wileyonlinelibrary.com.]

which ultimately helps in tissue regeneration. Actin filaments are shown in green color whereas nuclei in blue. Thre dimensional CLSM images depict cell penetration in 3D scaffold matrix up to ~50 μm and 70 μm on CS/nano β-TCP and CS/nano β-TCP/F composite scaffolds respectively from the surface of scaffolds as shown in Figure 4(C(b,d)). During initial days, blue color is prominent denoting less development of cytoskeleton. On the contrary, later day images show prominent green color confirming the extensive development of cytoskeleton as a result of increased cell proliferation as shown in Figure 3(a,b). CLSM images on 14th day [Figure 4(C(d))] also suggest that penetration of cells into the scaffold matrix is higher on fibrin conjugated samples than scaffolds without fibrin conjugation as reported earlier with alginate/β-TCP composite system.[43]

Osteogenic Differentiation of MSCs on Scaffolds

ALP Assay. Osteogenic potential of cell scaffold constructs was evaluated by ALP assay and illustrated in Figure 5(A). ALP activity is found to increase during the initial days of osteoblast differentiation since ALP is an early osteogenic marker. After 14 days of culture, a decrease in ALP activity is noticed. Among the developed scaffolds, MSCs on CS/nano-β TCP/F scaffold expresses higher ALP activity ($P < 0.05$) than cells that grow on CS and CS/nano β-TCP composite scaffold. There is no significant difference noticed during 14–21 days of difference among CS/nano β-TCP and CS/nano β-TCP/F composite scaffolds ($P > 0.05$). Increased levels of ALP on CS/nano β-TCP/F composite and CS/nano β-TCP composite scaffold scaffolds validate their support in differentiation of hMSCs into osteoblasts. Similar pattern of increase in ALP activity was observed in RGD conjugated hydrogels as reported earlier.[8]

In Vitro Mineralization Assay

Alizarin red assay was performed to assess the extent of matrix mineralization by differentiated cells on selected scaffolds. Figure 5(B) represents the optical microscopic images of Alizarin Red stained CS/nano β-TCP and CS/nano β-TCP/F composite scaffolds. On day 14 and 21, increased mineralization of CS/nano β-TCP/F scaffolds is observed in comparison to CS/nano β-TCP scaffolds. Further, the extent of mineralization was quantified and shown in Figure 5(C). Total calcium content of the scaffolds increased with time. On day 14, no significant difference is observed between the two samples. However, on day 21, both scaffold groups show a significant difference in mineralization ($P < 0.05$). Alizarin staining results are in good accordance with previous reports in which RGD conjugated CS showed greater mineralization compared to unmodified polymeric scaffolds.[4]

Expression of Osteogenic Specific Genes

Semi-quantitative RT-PCR was performed to assess the expression of osteoblast related genes at mRNA level for cells cultured

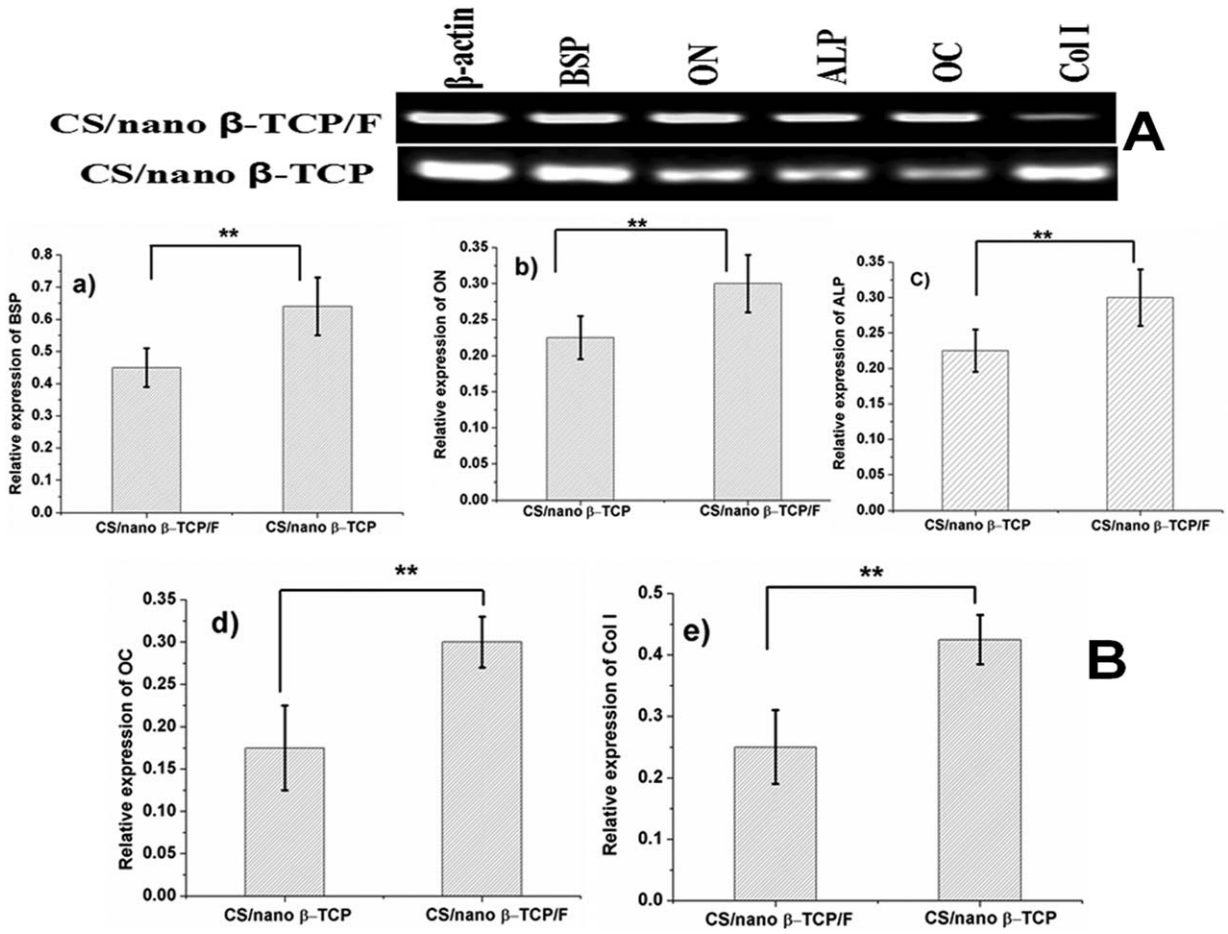

Figure 6. Images of amplified cDNA products (A) using specific osteogenic primers (BSP, ON, ALP, OC, and Col-I) for hMSCs cultured on CS/n β-TCP and CS/n β-TCP/F freeze-gelled composite scaffolds in osteogenic media for 21 days. Relative expression of BSP (a), ON (b), ALP (c), OC (d), and Col I (e) on mRNA of MSCs cultured on fibrin conjugated and non-conjugated composite scaffolds for 28 days of incubation.

for three weeks. The mRNA expression of genes such as ON, ALP, and OC was significantly higher in MSCs cultured on CS/nano β-TCP/F composite scaffold than non-conjugated ones as shown in Figure 6(A). The reason behind increase in gene expression may be attributed to synergic effect between β-TCP and fibrin which helped in increased differentiation of seeded cells.[44] The band intensities were further quantified to examine the relative expression of specific genes. Further, Figure 6(B) depicts the relative expression levels of the genes associated with osteogenic differentiation. A statistical difference ($P < 0.05$) was observed between scaffolds CS/nano β-TCP and CS/nanoβ-TCP/F in terms of gene expression. Similar increase in expression of osteoblast related markers was observed with rabbit MSCs seeded on fibrin coated β-TCP scaffolds as reported earlier.[43,45]

CONCLUSIONS

A novel fibrin conjugated CS/nano β-TCP composite scaffolds with well connected porous architecture were successfully prepared by freeze gelation method. A comparatively superior surface and mechanical property were achieved with fibrin conjugation when compared to non-conjugated CS/nano β-TCP composite scaffolds. Cytocompatibility by MTT, cell proliferation by DNA quantification, morphological analysis by FE-SEM, and confocal microscopy revealed that hMSCs were attached and well proliferated on the developed fibrin conjugated CS/nano β-TCP composite scaffolds. The scaffolds also exhibited enhanced MSCs proliferation and osteogenic differentiation property. Thus it has been demonstrated that developed fibrin conjugated CS/nano β-TCP freeze gelled porous composite scaffolds act as potential candidate for bone tissue regeneration.

ACKNOWLEDGMENTS

The authors are thankful to the National Institute of Technology, Rourkela and Department of Biotechnology, Govt. of India for providing institute fellowship to one of the authors (Siddiqui) and other necessary infrastructural facility to carry this work. The authors would also like to thank Dr. Anupam Banerjee for assisting in confocal microscopy at Department of biochemistry, University of Kolkata, India.

REFERENCES

1. Salgado, A. J.; Coutinho, O. P.; Reis, R. L. *Macromol. Biosci.* **2004**, *4*, 743.

2. Navarro, M.; Michiardi, A.; Castano, O.; Planell, J. *J. R Soc Interface* **2008**, *5*, 1137.
3. Di Martino, A.; Sittinger, M.; Risbud, M. V. *Biomaterials* **2005**, *26*, 5983.
4. Zhang, P.; Wu, H.; Wu, H.; Lu, Z.; Deng, C.; Hong, Z.; Jingand, X.; Chen, X. *Biomacromolecules* **2011**, *12*, 2667.
5. Yin, Y.; Ye, F.; Cui, J.; Zhang, F.; Li, X.; Yao, K. *J. Biomed. Mater. Res. A* **2003**, *67*, 844.
6. Siddiqui, N.; Pramanik, K. *J. Appl. Polym. Sci.* **2014**, *131*, 41025.
7. Rafat, M.; Li, F.; Fagerholm, P.; Lagali, N. S.; Watsky, M. A.; Munger, R.; Matsuura, T.; Griffith, M. *Biomaterials* **2008**, *29*, 3960.
8. Kang, S. W.; Kim, J. S.; Park, K. S.; Cha, B. H.; Shim, J. H.; Kim, J. Y.; Cho, D. W.; Rhie, J. W.; Lee, S. H. *Bone* **2011**, *48*, 298.
9. Deepachitra, R.; Chamundeeswari, M.; Krithiga, G.; Prabu, P.; Pandima Devi, M.; Sastry, T. P. *Carbon* **2013**, *56*, 64.
10. Zhou, W.; Zhao, M.; Zhao, Y.; Mou, Y. *J. Mater. Sci. Mater. Med.* **2011**, *22*, 1221.
11. Gamboa-Martinez, T.; Ribelles, J. G.; Ferrer, G. G. *J. Bioact. Compat. Polym.* **2011**, *26*, 464.
12. Han, C. M.; Zhang, L. P.; Sun, J. Z.; Shi, H. F.; Zhou, J.; Gao, C. Y. *J. Zhejiang Univ. Sci. B* **2010**, *11*, 524.
13. Tsai, W. B.; Chen, Y. R.; Liuand, H. L.; Lai, J. Y. *Carbohydr. Polym.* **2011**, *85*, 129.
14. Ahmed, T. A.; Dare, E. V.; Hincke, M. *Tissue Eng. B Rev.* **2008**, *14*, 199.
15. Shaikh, F. M.; Callanan, A.; Kavanagh, E. G.; Burke, P. E.; Grace, P. A.; McGloughlin, T. M. *Cells Tissues Organs* **2008**, *188*, 333.
16. Bhardwaj, N.; Chakraborty, S.; Kundu, S. C. *Int. J. Biol. Macromol.* **2011**, *49*, 260.
17. Grasman, J. M.; Page, R. L.; Dominko, T.; Pins, G. D. *Acta Biomater.* **2012**, *8*, 4020.
18. Causa, F.; Netti, P.; Ambrosio, L.; Ciapetti, G.; Baldini, N.; Pagani, S.; Martini, D.; Giunti, A. *J. Biomed. Mater. Res. A* **2006**, *76*, 151.
19. Jiang, T.; Abdel-Fattah, W. I.; Laurencin, C. T. *Biomaterials* **2006**, *27*, 4894.
20. Bi, L.; Cao, Z.; Hu, Y.; Song, Y.; Yu, L.; Yang, B.; Mu, J.; Huang, Z.; Han, Y. *J. Mater. Sci. Mater. Med.* **2011**, *22*, 51.
21. Kokubo, T.; Kushitani, H.; Sakka, S.; Kitsugi, T.; Yamamuro, T. *J. Biomed. Mater. Res.* **1990**, *24*, 721.
22. Cheng, K.; Kisaalita, W. S. *Biotechnol. Prog.* **2010**, *26*, 838.
23. Bissoyi, A.; Pramanik, K. *Cryoletters* **2013**, *34*, 453.
24. Xu, W.; Ma, J.; Jabbari, E. *Acta Biomater.* **2010**, *6*, 1992.
25. Hedley, D. W.; Friedlander, M. L.; Taylor, I. W.; Rugg, C. A.; Musgrove, E. A. *J. Histochem. Cytochem.* **1983**, *31*, 1333.
26. Gregory, C. A.; Grady Gunn, W.; Peister, A.; Prockop, D. *J. Anal Biochem.* **2004**, *329*, 77.
27. Marone, M.; Mozzetti, S.; De Ritis, D.; Pierelli, L.; Scambia, G. *Biol. Procedures Online* **2001**, *3*, 19.
28. Steward, R. L.; Cheng, C. M.; Jonathan, D. Y.; Bellin, R. M.; LeDuc, P. R. *Sci. Rep.* **2011**, 147.
29. Costa-Pinto, A. R.; Reis, R. L.; Neves, N. M. *Tissue Eng. B Rev.* **2011**, *17*, 331.
30. Spataru, M.; Tardei, C.; Nemtanu, M. R.; Bogdan, F. *Revue Roumaine de Chimie* **2008**, *53*, 955.
31. Zhang, Y.; Ni, M.; Zhang, M.; Ratner, B. *Tissue Eng.* **2003**, *9*, 337.
32. Lien, S. M.; Li, W. T.; Huang, T. J. *Mater. Sci. Eng. C* **2008**, *28*, 36.
33. Yilgor, P.; Sousa, R. A.; Reis, R. L.; Hasirci, N.; Hasirci, V. *J. Mater. Sci. Mater. Med.* **2010**, *21*, 2999.
34. Hsieh, C. Y.; Tsai, S. P.; Ho, M. H.; Wang, D. M.; Liu, C. E.; Hsieh, C. H.; Hsieh, H. J. *Carbohydr. Polym.* **2007**, *67*, 124.
35. Cao, Y.; Wang, B. *Int. J. Mol. Sci.* **2009**, *10*, 1514.
36. Helena, S.; Reis, R. Biodegradable Systems in Tissue Engineering and Regenerative Medicine; CRC Press: Boca Raton, FL, **2004**; 179.
37. Zhao, L.; Chang, J. *J. Mater. Sci. Mater. Med.* **2004**, *15*, 625.
38. Sarem, M.; Moztarzadeh, F.; Mozafari, M. *Carbohy. Polym.* **2013**, *93*, 635.
39. Stroncek, J. D.; Reichert, W. M. Indwelling Neural Implants: Strategies for contending with the In Vivo Environment; CRC Press: Boca Raton, FL, **2008**.
40. Adekogbe, I.; Ghanem, A. *Biomaterials* **2005**, *26*, 7241.
41. Jiang, L.; Li, Y.; Wang, X.; Zhang, L.; Wen, J.; Gong, M. *Carbohydr. Polym.* **2008**, *74*, 680.
42. Le Nihouannen, D.; Guehennec, L. L.; Rouillon, T.; Pilet, P.; Bilban, M.; Layrolle, P.; Daculsi, G. *Biomaterials* **2006**, *27*, 2716.
43. Diogo, G.; Gaspar, V.; Serra, I.; Fradique, R.; Correia, I. *Biofabrication* **2014**, *6*, 025001.
44. Mohammadi, Y.; Mirzadeh, H.; Moztarzadeh, F.; Soleimani, M.; Jabbari, E. *Iran. Polym. J.* **2007**, *16*, 57.
45. Zhao, H.; Ma, L.; Gao, C.; Wang, J.; Shen, J. *Mater. Sci. Eng. C* **2009**, *29*, 836.